

# MDSSD: Multi-scale Deconvolutional Single Shot Detector for small objects

Lisha Cui

Zhengzhou University, No.100 Kexue Road, Zhengzhou 450000, China

**Abstract.** In order to improve the detection accuracy for objects at different scales, most of the recent works utilize the pyramidal feature hierarchy of the ConvNets from bottom to top. Nevertheless, the bottom features are poor in detection due to less semantic information, especially for small objects. For the top semantic features, most of the fine details for small objects are lost. In this paper, we design a Multi-scale Deconvolutional Single Shot Detector for small objects (MDSSD for short). To obtain the feature maps with enriched representation power, we add the high-level features with rich semantic information to the low-level features via deconvolution Fusion Block. It is noteworthy that multiple high-level features with different scales are upsampled simultaneously in our framework. We implement the skip connections to form more descriptive feature maps and predictions are made on these new fusion features. Our proposed framework achieves 78.6% mAP on PASCAL VOC2007 test and 26.8% mAP on MS COCO test-dev2015 at 38.5 FPS with only  $300 \times 300$  input.

**Keywords:** Object detection, multi-scale deconvolution, fusion block, small objects, real-time

## 1 Introduction

Object detection has always been the focus and challenge in the field of computer vision, including the detection for small objects. To recognize objects at various scales, the majority of previous works based on hand-crafted features [1,2] utilize image pyramids as input (Figure 1(a)). Those works are expensive considering memory and inference time. By using deep convolutional networks (ConvNets [?]), the performance of object detection has been improved significantly. However, small object detection is still a challenging issue due to low resolution and noisy representation in images.

The scale problem will directly affect the detection accuracy. In recent years, the hand-engineered features have been replaced with features computed by convolutional neural networks. Recent detection systems [3,4,5] leverage the top-most feature map computed by ConvNets on a single input scale to predict candidate bounding boxes with different scales and aspect ratios (Figure 1(b)). However, the top-most feature map has the fixed receptive field, which is conflict with objects at different scales in natural images. In particular, there will be little information left on the top-most feature for small objects, therefore it may compromise object detection performance.

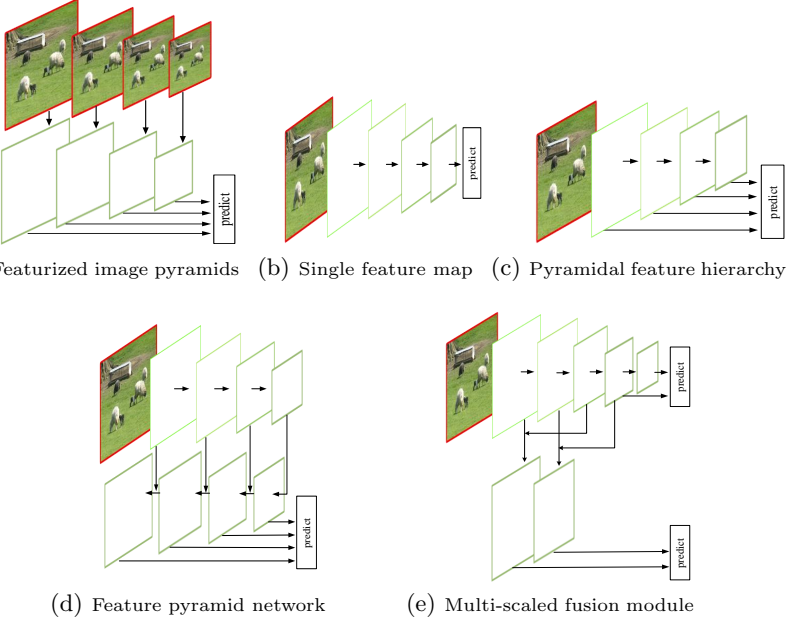


**Fig. 1.** (a) Using image pyramids as input to compute a multi-scale feature representation, which is computationally expensive. (b) Using only single scale feature to make predictions. (c) Using pyramidal feature hierarchy to replace featurized image pyramids. (d) A top-down architecture with lateral connections. (e) Our proposed multi-scale fusion module with skip connections

The methods, such as SSD [6] and MS-CNN [7], utilize the pyramidal feature hierarchy from bottom to top (Figure 1(c)). They utilize multiple feature maps with different resolutions to naturally handle objects of various sizes. Nevertheless, the layers from the bottom ConvNets have weak semantic information, which will harm their representational capacity for small object recognition. The most recent works [8,9] try to observe and utilize the pyramidal features to a large extent by building a top-down architecture with lateral connections (Figure 1(d)). These networks show dramatic improvements in accuracy of conventional detectors, especially for small objects. However, they implement connections for every prediction module. And more additional layers lead to more computational cost at the same time, making it impractical for real application considering the inference time.

In this paper, we aim to improve the detection performance for small objects and maintain the inference speed at the same time. The low-level features of a ConvNet are more accurate for object location due to small receptive fields and less downsampling. Nevertheless, the weak semantic information makes the low-level features poor in classification, especially for small objects. With this in mind, we add the high-level features with semantic information to the low-level features via deconvolution Fusion Block to obtain the feature maps with rich in-

formation (Figure 1(e)). We take the state-of-the-art object detector, Single Shot Multibox Detector, as the base framework, and then add multi-scale deconvolution fusion module. We proposed the Multi-scale Deconvolutional Single Shot Detector for small objects, named MDSSD. Unlike FPN [8] and DSSD [9], we do not only upsample the top-most feature. Instead, multiple high-level features with different spatial resolutions are upsampled simultaneously, then we merge them with some of the bottom features to form more semantic feature maps. Small kernels are applied on the fusion features to produce either a score for a category or a shape offset. In order to improve the performance of deep neural network for small objects, we add the lower feature output by the backbone network for prediction purposely. To avoid additional cost we only conduct Fusion Module for the bottom features and there is no operation to the top features. The proposed MDSSD framework turns out to be rather influential for small objects, and it can meet the real-time application as well.

The main contributions of our work are summarized as follows:

(1) We propose a novel feature fusion framework for object detection. Several deconvolution layers are applied to the semantic high-level features from different depth, hallucinating higher resolution features. And then we merge them with the low-level features to achieve skip connections.

(2) We delicately design several multi-scale deconvolution Fusion Modules. The new fusion modules are rich in semantic information with relatively large resolution, providing a significant boost on detection of small objects.

(3) By conducting quantitative and qualitative experiments on benchmark dataset of PASCAL VOC2007 and MS COCO, we prove that the proposed MDSSD is superior to the conventional SSD. Moreover, it improve the performance for small objects with a large margin and a slightly degraded speed.

## 2 Related Work

Most of traditional methods for object detection are based on the sliding-window paradigm, using the hand-crafted features, such as Haar [10] and DPM [11]. With the development of deep ConvNets in recent years, the accuracy and inference speed of detection have been greatly improved by integrating feature learning and classifier into a framework. We classify these works based on ConvNets into the following three categories:

**The detectors based on the top-most feature of convolutional neural network.** OverFeat [12] applies a sliding window to the feature map to create bounding boxes, decomposing the detection into localization and classification. It tends to be costly. SPPnet [5] designs the Spatial Pyramid Pooling layer so that the input images of any size are feasible, which is efficient in computation. R-CNN [13] and Fast R-CNN [3] use selective search to generate bounding boxes, extracting features with CNN and classifying them by SVM. Faster R-CNN [4] uses RPN (Region Propose Network) to directly generate the anchor boxes with different scales and aspect ratios on the feature maps, which improves effectiveness and efficiency. YOLO [14] divides the input image into  $n$  regions, and then

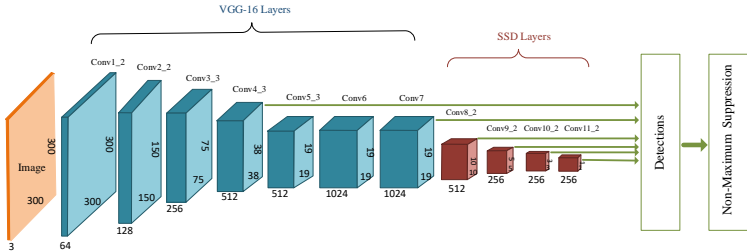


**Fig. 2.** The architecture of SSD [6]

regresses and classifies the bounding boxes in each region at real-time speed. However, all these methods are based on the top-most feature of convolutional neural network to locate and classify the objects. It relies on the information extracted by the upper feature to a large extent and does not make full use of the bottom details.

**The detectors based on multi-scale features of convolutional neural network.** To make full use of the multifarious information from different convolution layers to cover the objects with different scales and shapes, a set of approaches [6,7,15,16] make predictions on multi-scale features. SSD [6] is a single shot detector, which makes predictions by using small convolutional filters of  $3 \times 3$  on six features at different depths from bottom to top. It is one of state-of-the-art detectors considering both accuracy and speed. MS-CNN [7] proposes a framework which consists of a proposal sub-network and a detection sub-network. In the proposal sub-network, detection is performed at multiple output features. Deconvolution layer is introduced to upsample feature maps and add contextual information. Nevertheless, the layers from the bottom of a ConvNet have weak semantic information, which will harm their representational capacity for small object recognition.

**The detectors based on combinations of multi-layer features of convolutional neural network.** In order to enrich the feature maps, a number of approaches [17,18,19,20,21] concatenate multi-scale features of ConvNets to increase context information. The recent methods, FPN [8] and TDM [22], adopt top-down pathway and conduct skip connections in their architectures, which enhances the power of features. DSSD [9] applies deconvolution layer to the top of SSD to realize upsampling and then achieves integrating information from earlier feature maps. Predictions are made on these new fusion feature maps with context information. These bottom-up and top-down architecture are also utilized on semantic segmentation [24], and human pose estimation [23].

Inspired by these researches, we propose MDSSD for small object detection. It combines high-level and low-level feature maps to add contextual information for small object detection. The difference is that our deconvolution layers are not applied to the top-most of the ConvNet, but on multiple top features with different scales simultaneously. Then we merge them with some bottom layers to form new feature maps which are more informative.

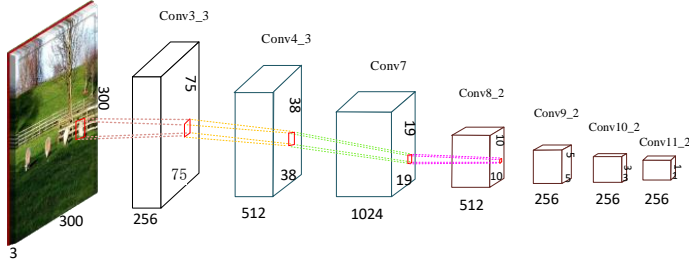


**Fig. 3.** Detecting small objects such as the sheep in the image requires the fine details from the shallow layers. The area of the sheep is about  $30 \times 30$ , and it only remains  $1 \times 1$  on conv8.2. As for smaller objects, the representation of details will be totally lost after conv7 layer

### 3 Multi-scale Deconvolutional Network

In this section, we first review the powerful SSD framework briefly. Then we introduce the principle of the proposed Multi-scale Deconvolutional Single Shot Detector. Next, a detailed analysis of Fusion Block is given. Finally, we discuss the training policy.

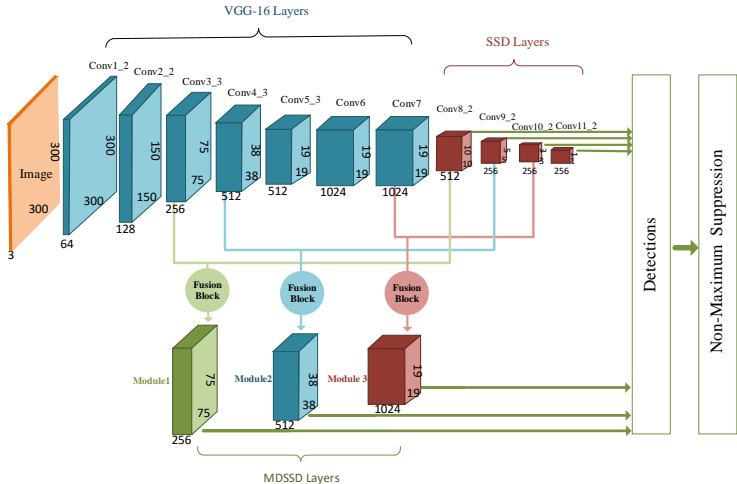
#### 3.1 SSD

Figure 2 is the overall architecture of SSD with  $300 \times 300$  input. It takes the standard VGG16 [25] as feature extractor, and adds extra convolutional layers to the truncated backbone network. SSD utilizes the pyramidal feature hierarchy within a ConvNet to predict objects with different scales. Predictions at multiple scales improve the mAP, while single-shot architecture achieves real-time requirements. However, it is hard for SSD to classify the small objects owing to the weak semantic information on the shallow features. Therefore, it is imperative to yield more semantic feature maps for small object detection.

#### 3.2 MDSSD Architecture

We empirically define that an object is small if its area is less than  $32 \times 32$  (area is measured as the number of pixels in the segmentation mask). As shown in Figure 3, the area of a sheep is about  $30 \times 30$ , and we could obtain the fine details only in the early layers of the ConvNet (before conv7 layer). The representation of details for the sheep will be totally lost in the coarse, semantic deeper layers (after conv7 layer). That is, shallow feature maps inherently have small receptive fields, and they are beneficial for detecting small objects. Therefore, it is significant to make full use of the low-level feature maps for detection of small and extra-small objects.

Nevertheless, shallow feature maps have poor semantic information, which may compromise object detection performance, especially for small objects. In



**Fig. 4.** The architecture of MDSSD. First we apply deconvolution layers to the high-level semantic feature maps at different scales (i.e., conv8\_2, conv9\_2, and conv10\_2) simultaneously. Then we build skip connections with lower-layers (conv3\_3, conv4\_3, and conv7) through Fusion Block and form 3 new fusion layers (Module 1, Module 2, and Module 3). Predictions are made on both the new fusion layers (Module 1, Module 2, and Module 3) and the original SSD layers (conv8\_2, conv9\_2, conv10\_2, and conv11\_2) at the same time

order to obtain the feature maps with enriched representation power for object detection, we combine the high-level features with the low-level ones. The fusion features are rich in both local and global information.

Figure 4 is the overall framework of MDSSD for  $300 \times 300$  input. Different from other fusion networks, we apply upsampling operation not just to the top-most layer of the network, but across multiple top layers. Through Fusion Block, conv9\_2 and conv10\_2 are upsampled and then we merge them with conv4\_3 and conv7, respectively. The new fusion feature maps, named Module 2 and Module 3, will replace the original conv4\_3 and conv7 of SSD to predict objects. In order to improve the performance of small object detection, it is necessary to make full use of underlying feature maps. Therefore, we add Module 1 which connects the low-level feature (conv3\_3) and high-level feature (conv8\_2) to make prediction.

In summary, we have 7 prediction feature maps in total, including 3 fusion modules (Module 1, Module 2, and Module 3) and 4 original SSD feature maps (conv8\_2, conv9\_2, conv10\_2, and conv11\_2). Then we apply  $3 \times 3 \times p$  ( $p$  is the channels for a feature) small kernels to produce the score and shape offset for a specific bounding box. Non-maximum suppression (nms) with a confidence threshold of 0.01 and jaccard overlap of 0.45 is performed to filter out most of the bounding boxes during inference. Finally, we retain the top 200 detections.



**Table 1.** The structure of three Fusion Blocks with  $300 \times 300$  and  $512 \times 512$  input.  $[\cdot] \times 2$  indicates double identical operations. The stride is 2 for all deconvolution layers, and 1 for convolution layers

Fusion Module	Module 1		Module 2		Module 3	
Connection Layers	conv3_3	conv8_2	conv4_3	conv9_2	conv7	conv10_2
Structure $300 \times 300$	3 $\times$ 3 $\times$ 256 Conv L2 Norm	$\begin{bmatrix} 2 \times 2 \times 256 \text{ Deconv} \\ 3 \times 3 \times 256 \text{ Conv} \\ \text{Relu} \end{bmatrix} \times 2$ $3 \times 3 \times 256 \text{ Deconv}$ $3 \times 3 \times 256 \text{ Conv}$ L2 Norm	3 $\times$ 3 $\times$ 512 Conv L2 Norm	$\begin{bmatrix} 2 \times 2 \times 256 \text{ Deconv} \\ 3 \times 3 \times 256 \text{ Conv} \\ \text{Relu} \end{bmatrix} \times 2$ $2 \times 2 \times 512 \text{ Deconv}$ $3 \times 3 \times 512 \text{ Conv}$ L2 Norm	3 $\times$ 3 $\times$ 1024 Conv L2 Norm	$\begin{bmatrix} 2 \times 2 \times 512 \text{ Deconv} \\ 3 \times 3 \times 512 \text{ Conv} \\ \text{Relu} \end{bmatrix} \times 2$ $3 \times 3 \times 1024 \text{ Deconv}$ $3 \times 3 \times 1024 \text{ Conv}$ L2 Norm
Structure $512 \times 512$	3 $\times$ 3 $\times$ 256 Conv L2 Norm	$\begin{bmatrix} 2 \times 2 \times 256 \text{ Deconv} \\ 3 \times 3 \times 256 \text{ Conv} \\ \text{Relu} \end{bmatrix} \times 2$ $2 \times 2 \times 256 \text{ Deconv}$ $3 \times 3 \times 256 \text{ Conv}$ L2 Norm	3 $\times$ 3 $\times$ 512 Conv L2 Norm	$\begin{bmatrix} 2 \times 2 \times 256 \text{ Deconv} \\ 3 \times 3 \times 256 \text{ Conv} \\ \text{Relu} \end{bmatrix} \times 2$ $2 \times 2 \times 512 \text{ Deconv}$ $3 \times 3 \times 512 \text{ Conv}$ L2 Norm	$\begin{bmatrix} 2 \times 2 \times 512 \text{ Deconv} \\ 3 \times 3 \times 512 \text{ Conv} \\ \text{Relu} \end{bmatrix} \times 2$ $2 \times 2 \times 1024 \text{ Deconv}$ $3 \times 3 \times 1024 \text{ Conv}$ L2 Norm	
Fusion	Eltw-sum Relu 3 $\times$ 3 $\times$ 256 Conv Relu		Eltw-sum Relu 3 $\times$ 3 $\times$ 512 Conv Relu		Eltw-sum Relu 3 $\times$ 3 $\times$ 1024 Conv Relu	

**Default Boxes.** Figure 4 shows the details of MDSSD with  $300 \times 300$  input model. For Module 2 and Module 3 in MDSSD, the scales and aspect ratios of default boxes are consistent with conv4\_3 and conv7 in SSD, respectively. The scale of Module 2 is set to 0.2, and the scale of the highest layer is 0.9. Default boxes with aspect ratios of 1, 2, 3,  $\frac{1}{2}$ , and  $\frac{1}{3}$  are generated to match different objects. For Module 2, conv10\_2, and conv11\_2, each cell of the feature maps predicts four default boxes. Others have six default boxes for each location. As for Module 1 we add, we keep them the same as Module 2 both in scale and aspect ratio. Following the strategy in SSD, we add extra conv12\_2 for  $512 \times 512$  input model to make prediction.

**Matching and Hard Negative Mining.** We match each ground truth box to the default box with the best jaccard overlap. Then we match default boxes to any ground truth with jaccard overlap higher than a threshold (0.5). This strategy is beneficial to predict multiple bounding boxes with high scores for overlapped objects. The negative samples with top loss value are selected from the non-matched default boxes so that the ratio of positive and negative samples is 1:3.

**Loss Function.** The training objective is the weighted sum between localization loss (Smooth L1 [3]) and confidence loss (Softmax). More details can be found in [6].

## 4 Experimental Results

We evaluate MDSSD on benchmark datasets, PASCAL VOC2007 [26] and MS COCO [27]. All the experiments are implemented in Caffe [28] on the machine with two 1080Ti GPUs. We use the well-trained SSD model as the pre-trained

**Table 2.** PASCAL VOC2007 test results. SSD300\* and SSD512\* indicate the latest version updated by the authors. All the methods are trained on VOC2007 and VOC2012 trainval, and test on VOC2007 test

Method	network	mAP	aero	bike	bird	boat	bottlebus	car	cat	chair	cow	table	dog	horse	mbike	person	plant	sheep	sofa	train	tv	
Faster[4]	VGG	73.2	76.5	79.0	70.9	65.5	52.1	83.1	84.7	86.4	52.0	81.9	65.7	84.8	84.6	77.5	76.7	38.8	73.6	73.9	83.0	72.6
ION[18]	VGG	75.6	79.2	83.1	77.6	65.6	54.9	85.4	85.1	87	54.4	80.6	73.8	85.3	82.2	82.2	74.4	47.1	75.8	72.7	84.2	80.4
Faster[29]	Residual-101	76.4	79.8	80.7	76.2	68.3	55.9	85.1	85.3	<b>89.8</b>	56.7	87.8	69.4	88.3	88.9	80.9	78.4	41.7	78.6	79.8	85.3	72.0
MR-CNN[7]	VGG	78.2	80.3	84.1	78.5	70.8	68.5	88.0	85.9	87.8	60.3	85.2	73.7	87.2	86.5	85.0	76.4	48.5	76.3	75.5	85.0	<b>81.0</b>
R-FCN[30]	Residual-101	80.5	79.9	87.2	81.5	72.0	<b>69.8</b>	86.8	88.5	<b>89.8</b>	<b>67.0</b>	<b>88.1</b>	74.5	<b>89.8</b>	90.6	79.9	81.2	53.7	81.8	81.5	85.9	79.9
SSD300*[6]	VGG	77.5	79.5	83.9	76.0	69.6	50.5	87.0	85.7	88.1	60.3	81.5	77.0	86.1	87.5	83.9	79.4	52.3	77.9	79.5	<b>87.6</b>	<b>76.8</b>
SSD512*[6]	VGG	79.5	84.8	85.1	81.5	73.0	57.8	87.8	88.3	87.4	63.5	85.4	73.2	86.2	86.7	83.9	82.5	55.6	81.7	79.0	86.6	80.0
DSSD321[9]	Residual-101	78.6	81.9	84.9	80.5	68.4	53.9	85.6	86.2	88.9	61.1	83.5	78.7	86.7	88.7	86.7	79.7	51.7	78.0	80.9	87.2	79.4
DSSD513[9]	Residual-101	<b>81.5</b>	86.6	86.2	82.6	<b>74.9</b>	62.5	<b>89.0</b>	88.7	88.8	65.2	87.0	<b>78.7</b>	88.2	89.0	87.5	<b>83.7</b>	51.1	<b>86.3</b>	<b>81.6</b>	85.7	83.7
MDSSD300	VGG	78.6	86.5	87.6	78.9	70.6	55.0	86.9	87.0	88.1	58.5	84.8	73.4	84.8	89.2	88.1	78.0	52.3	78.6	74.5	86.8	80.7
MDSSD512	VGG	80.3	<b>88.8</b>	<b>88.7</b>	<b>83.2</b>	73.7	58.3	88.2	<b>89.3</b>	87.4	62.4	85.1	75.1	84.7	<b>89.7</b>	<b>88.3</b>	83.2	<b>56.7</b>	84.0	77.4	83.9	77.6

model for MDSSD training. Then we fine-tune our model on PASCAL VOC and MS COCO. The performance is measured by mean average precision (mAP) on VOC2007 test and COCO test-dev2015 datasets. We compare the results with state-of-the-art deep convolutional networks about the mAP and inference speed.

#### 4.1 PASCAL VOC2007

We train MDSSD on PASCAL VOC2007 and VOC2012 trainval (i.e. 07+12, 16551 images), and test on VOC2007 test (4952 images). Batch size is set to 32 for  $300 \times 300$  input and 12 for  $512 \times 512$  input. We use  $10^{-3}$  learning rate for the first  $60k$  iterations, then decrease it to  $10^{-4}$  for the next  $40k$  iterations and continue training for another  $20k$  iterations with  $10^{-5}$ . The momentum and weight decay are set to 0.9 and 0.0005 respectively by using SGD.

Table 2 shows our detection results on VOC2007 test compared with other state-of-the-art architectures. Our model with  $300 \times 300$  input has achieved 78.6% mAP. It is superior to the latest SSD300\* by 1.1 points and can be comparable to DSSD321 with  $321 \times 321$  input. By increasing input size to  $512 \times 512$ , MDSSD achieves a better performance, improving SSD512\* from 79.5 to 80.3. It has outperformed most of the other deep networks. The mAP of DSSD513 is higher than MDSSD512, which may owe to ResNet-101. DSSD utilizes for the backbone network. However, it should be noted that MDSSD512 is much faster than DSSD513, as can be observed in Table 4.

Our MDSSD300 model shows significant improvement compared to SSD300 model, while the MDSSD512 model outperforms SSD512 with a small margin.

In order to verify the performance of MDSSD for small objects, we also utilize the detection analysis tool from [31]. Figure 6 shows the contrast of MDSSD and SSD for sensitivity and impact of object size. It is obvious that the performance of MDSSD has improved, especially for the extra small and small objects. Compared with the SSD300 and SSD512 model, our MDSSD300 model shows more significant improvement than MDSSD512 model. We consider that this performance proves the effectiveness of our model for small objects once again.

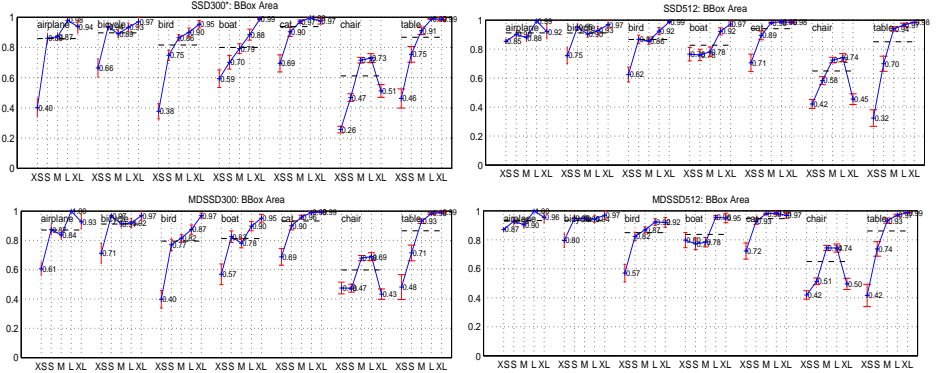


**Fig. 6.** Sensitivity and impact of object size on VOC2007 test set using [31]. The top row shows the latest SSD results of BBox Area per category for 300 input and 512 input model, and the bottom row shows our results. Key: BBox Area: XS=extra-small; S=small

The performance of some specific classes improves significantly as well, such as airplane with the background of sky. This may benefit from the fusion module with context information.

We also use the initial weights model pre-trained on the ILSVRC CLS-LOC dataset [32] for MDSSD training, however we do not see any accuracy improvement but double training time.

## 4.2 MS COCO

To further validate our MDSSD model, we train MDSSD300 and MDSSD512 on MS COCO [27]. We use the `trainval35` [18] set (118287 images) for training and evaluate the results on the standard `test-dev2015` split (20288 images). The batch size is set to 32 for 300 input and 16 for 512 input. We train the model with  $10^{-3}$  for the first 160k iterations, then  $10^{-4}$  and  $10^{-5}$  for another 120k and 40k iterations. The total number of training iterations is 320k.

**Table 3.** MS COCO `test-dev2015` detection results

Method	data	network	Avg. Precision, IoU: 0.5 0.95 0.5 0.75	Avg. Precision, Area: S M L			Avg. Recall, #Dets: 1 10 100			Avg. Recall, Area: S M L		
				1	10	100	1	10	100	1	10	100
Faster [4]	trainval	VGGNet	21.9 42.7 -	-	-	-	-	-	-	-	-	-
ION [18]	train	VGGNet	23.6 43.2 23.6	6.4	24.1	38.3	23.2	32.7	33.5	10.1	37.7	53.6
Faster [29]	trainval	Residual-101	34.9 55.7 37.4	15.6	38.7	50.9	-	-	-	-	-	-
R-FCN [30]	trainval	Residual-101	29.9 51.9 -	10.8	32.8	45.0	-	-	-	-	-	-
SSD300* [6]	trainval35k	VGGNet	25.1 43.1 25.8	6.6	25.9	41.4	23.7	35.1	37.2	11.2	40.4	58.4
SSD512* [6]	trainval35k	VGGNet	28.8 48.5 30.3	10.9	31.8	43.5	26.1	39.5	42.0	16.5	46.6	60.8
DSSD321 [9]	trainval35k	Residual-101	28.0 46.1 29.2	7.4	28.1	47.6	25.5	37.1	39.4	12.7	42.0	62.6
DSSD513 [9]	trainval35k	Residual-101	33.2 53.3 35.2	13.0	35.4	51.1	28.9	43.5	46.2	21.8	49.1	66.4
DSOD300 [15]	trainval	DS/64-192-48-1	29.3 47.3 30.6	9.4	31.5	47.0	27.3	40.7	43.0	16.7	47.1	65.0
MDSSD300	trainval35k	VGGNet	26.8 45.9 27.7	10.8	27.5	40.8	24.3	36.6	38.8	15.8	42.3	56.3
MDSSD512	trainval35k	VGGNet	30.1 50.5 31.4	13.9	31.4	43.6	26.3	40.3	42.9	22.4	44.2	60.0

To obtain results on COCO `test-dev2015`, for which the ground-truth annotations are hidden, we upload generated results to the evaluation server. Table 3 shows the details. We observe that MDSSD300 achieves 26.8% mAP@[0.5:0.95], 45.9% mAP@0.5, and 27.7% mAP@0.75, which are superior to the conventional SSD300. MDSSD512 also outperforms the baseline SSD512. Even though our model does not perform as well as DSSD, it should be noticed that the backbone network of MDSSD is VGG16 and MDSSD is about 4 times faster than DSSD. Compared to the other detectors based on VGG16 such as Faster R-CNN [4] and ION [18] with  $1000 \times 600$  input, MDSSD achieve the best results.

What is noteworthy is that AP of MDSSD for small objects (area  $<32^2$ ) is 10.8%/13.9%, which is higher than that of SSD (6.6%/10.9%), DSSD (7.4%/13%), and DSOD (9.4%) with a large margin. It outperforms all state-of-the-art networks both based on VGG16 and Residual-101. Our method achieves a higher AR (average recall) for small objects as well, which prove that MDSSD is more powerful on detection of small objects.

**Table 4.** Comparison of Speed and Accuracy on PASCAL VOC2007 dataset. All the methods are trained on the union of VOC2007 and VOC2012 `trainval` and tested on VOC2007 `test`

Method	backbone network	GPU	Input Size	speed(FPS)	mAP(%) VOC2007
Faster[4]	VGG16	Titan X	$\sim 1000 \times 600$	7	73.2
Faster[29]	Residual-101	K40	$\sim 1000 \times 600$	2.4	76.4
R-FCN [30]	Residual-101	Titan X	$\sim 1000 \times 600$	9	80.5
SSD300*[6]	VGG16	Titan X	$300 \times 300$	46	77.5
SSD512*[6]	VGG16	Titan X	$512 \times 512$	19	79.8
SSD300*[6]	VGG16	1080Ti	$300 \times 300$	64.5	77.5
SSD512*[6]	VGG16	1080Ti	$512 \times 512$	33.8	79.5
DSSD321[9]	Residual-101	Titan X	$321 \times 321$	9.5	78.6
DSSD513[9]	Residual-101	Titan X	$513 \times 513$	5.5	81.5
DSOD300[15]	DS/64-192-48-1	Titan X	$300 \times 300$	17.4	77.7
MDSSD300	VGG16	1080Ti	$300 \times 300$	38.5	78.6
MDSSD512	VGG16	1080Ti	$512 \times 512$	17.3	80.3

### 4.3 Inference Time

New parameters need to be learned due to additional layers in MDSSD, so the inference time of the network will be impaired. We use 2000 images with batch size 1 to evaluate the inference speed of MDSSD on a machine with a Nvidia 1080Ti GPU. The results are presented in the 5th column of Table 4, including other state-of-the-art methods. For fair comparison, we verify SSD on the same

single Nvidia 1080Ti GPU as well. Our model runs at 38.5 FPS with  $300 \times 300$  input and 17.3 FPS with  $512 \times 512$  input, respectively. Although the speed is lower than SSD, it can still meet the real-time application. Our method exceeds the two-stage networks with a large margin in speed, and it can also outperform one-stage methods, DSSD and DSOD. It is mainly because we only add context information to the bottom layers and there is no operation on the top layers.

#### 4.4 Qualitative Results

Figure 7 and Figure 8 show some qualitative results on PASCAL VOC2007 test and COCO test-dev2015. We only display the bounding boxes with the score larger than 0.6. Different colors of the bounding boxes indicate different object categories.

Our model performs better than conventional SSD in two cases. The first one is in scenes containing small or occluded objects as shown in Figure 7, and the second one is in scenes containing contextual information as shown Figure 8. The detection of the objects with specific relationship is mutual. For example, the detection for motorbike can be beneficial to detect person on it as can be observed in Figure 8(a). We owe that to the multi-scale fusion modules with semantic information designed in Figure 4.

There are still some false and omissive detections in our visualized results. Some examples are given in Figure 9 and Figure 10. It may be caused by objects truncation and images obscure.

### 5 Conclusions

This paper proposes a multi-scale deconvolutional single shot detector. We use multiple feature maps to better match various objects with different scales and aspect ratios. The skip connections add contextual information to low-level feature maps and make them more descriptive. Experiments demonstrate the effectiveness of MDSSD for small objects. It outperforms the state-of-the-art methods with higher mAP and comparable detection speed. While we only take SSD as the base architecture in our method, the principle can be also applied to other object detectors, such as Faster R-CNN [4]. It is imperative that the feature extractor can be replaced from VGG to a more effective network, such as ResNet [29] and DenseNet [33], which will be the future work.



(a) The scenes containing small or occluded objects test on PASCAL VOC2007 test



(b) The scenes containing small or occluded objects test on COCO test-dev2015

**Fig. 7.** The detection results of MDSSD (column 2, column 4, and column 6) compared with SSD (column 1, column 3, and column 5) in scenes containing small or occluded objects. We can see that MDSSD yields better performance on small and occluded objects both in (a) and (b)



(a) The scenes containing contextual information test on PASCAL VOC2007 test



(b) The scenes containing contextual information test on COCO test-dev2015

**Fig. 8.** The detection results of MDSSD (column 2, column 4, and column 6) compared with SSD (column 1, column 3, and column 5) in scenes containing contextual information. The results of classes with specific relationships can be improved: kid and chair, dog and sofa, motorbike and person on motorbike in (a), football and football player, surfboard and surfer, baseball and baseball plater in (b).



**Fig. 9.** The false detections of MDSSD on PASCAL VOC2007 test with the score higher than 0.6



**Fig. 10.** The omitted detections of MDSSD on PASCAL VOC2007 test with the score higher than 0.6

## References

1. Dalal, N., Triggs, B.: Histograms of oriented gradients for human detection. In: Computer Vision and Pattern Recognition. (2005)
2. Lowe, D.G., Lowe, D.G.: Distinctive image features from scale-invariant keypoints. International Journal of Computer Vision **60**(2) (2004) 91–110
3. Girshick, R.: Fast r-cnn. In: International Conference on Computer Vision. (2015)
4. Ren, S., He, K., Girshick, R., Sun, J.: Faster r-cnn: towards real-time object detection with region proposal networks. In: International Conference on Neural Information Processing Systems. (2015)
5. He, K., Zhang, X., Ren, S., Sun, J.: Spatial pyramid pooling in deep convolutional networks for visual recognition. In: European Conference on Computer Vision. (2014)
6. Liu, W., Anguelov, D., Erhan, D., Szegedy, C., Reed, S., Fu, C.Y., Berg, A.C.: Ssd: Single shot multibox detector. In: European Conference on Computer Vision. (2016)
7. Cai, Z., Fan, Q., Feris, R.S., Vasconcelos, N.: A unified multi-scale deep convolutional neural network for fast object detection. In: European Conference on Computer Vision. (2016)
8. Lin, T.Y., Dollr, P., Girshick, R., He, K., Hariharan, B., Belongie, S.: Feature pyramid networks for object detection. In: Computer Vision and Pattern Recognition. (2017)
9. Fu, C.Y., Liu, W., Ranga, A., Tyagi, A., Berg, A.C.: Dssd : Deconvolutional single shot detector. arXiv preprint arXiv:1701.06659 (2017)
10. Viola, P., Jones, M.: Rapid object detection using a boosted cascade of simple features. In: Computer Vision and Pattern Recognition. (2001)
11. Felzenszwalb, P.F., Girshick, R.B., Mcallester, D., Ramanan, D.: Object detection with discriminatively trained part-based models. IEEE Transactions on Pattern Analysis and Machine Intelligence **47**(2) (2014) 6–7
12. Sermanet, P., Eigen, D., Zhang, X., Mathieu, M., Fergus, R., Lecun, Y.: Overfeat: Integrated recognition, localization and detection using convolutional networks. In: International Conference on Learning Representations. (2014)
13. Girshick, R., Donahue, J., Darrell, T., Malik, J.: Rich feature hierarchies for accurate object detection and semantic segmentation. In: Computer Vision and Pattern Recognition. (2014)
14. Redmon, J., Divvala, S., Girshick, R., Farhadi, A.: You only look once: Unified, real-time object detection. In: Computer Vision and Pattern Recognition. (2016)
15. Shen, Z., Liu, Z., Li, J., Jiang, Y.G., Chen, Y., Xue, X.: Dsod: Learning deeply supervised object detectors from scratch. In: International Conference on Computer Vision. (2017)
16. Shrivastava, A., Sukthankar, R., Malik, J., Gupta, A.: Beyond skip connections: Top-down modulation for object detection. CoRR **abs/1612.06851** (2016)
17. Kong, T., Yao, A., Chen, Y., Sun, F.: Hypernet: Towards accurate region proposal generation and joint object detection. In: Computer Vision and Pattern Recognition. (2016)
18. Bell, S., Zitnick, C.L., Bala, K., Girshick, R.: Inside-outside net: Detecting objects in context with skip pooling and recurrent neural networks. In: Computer Vision and Pattern Recognition. (2016)
19. Liu, W., Rabinovich, A., Berg, A.C.: Parsenet: Looking wider to see better. arXiv preprint arXiv:1506.04579 (2015)

20. Redmon, J., Farhadi, A.: Yolo9000: Better, faster, stronger. In: Computer Vision and Pattern Recognition. (2017)
21. Honari, S., Yosinski, J., Vincent, P., Pal, C.: Recombinator networks: Learning coarse-to-fine feature aggregation. In: Computer Vision and Pattern Recognition. (2016)
22. Shrivastava, A., Sukthankar, R., Malik, J., Gupta, A.: Beyond skip connections: Top-down modulation for object detection. CoRR **abs/1612.06851** (2016)
23. Newell, A., Yang, K., Deng, J.: Stacked hourglass networks for human pose estimation. In: European Conference on Computer Vision. (2016)
24. Pinheiro, P.O., Lin, T.Y., Collobert, R., Dollr, P.: Learning to refine object segments. In: European Conference on Computer Vision. (2016)
25. Simonyan, K., Zisserman, A.: Very deep convolutional networks for large-scale image recognition. In: International Conference on Learning Representations. (2015)
26. Everingham, M., Gool, L., Williams, C.K., Winn, J., Zisserman, A.: The pascal visual object classes (voc) challenge. International Journal of Computer Vision **88**(2) (2010) 303–338
27. Lin, T.Y., Maire, M., Belongie, S., Hays, J., Perona, P., Ramanan, D., Dollr, P., Zitnick, C.L.: Microsoft coco: Common objects in context. In: European Conference on Computer Vision. (2014)
28. Jia, Y., Shelhamer, E., Donahue, J., Karayev, S., Long, J., Girshick, R., Guadarrama, S., Darrell, T.: Caffe: Convolutional architecture for fast feature embedding. In: Acm International Conference on Multimedia. (2014)
29. He, K., Zhang, X., Ren, S., Sun, J.: Deep residual learning for image recognition. In: Computer Vision and Pattern Recognition. (2016)
30. Dai, J., Li, Y., He, K., Sun, J.: R-fcn: Object detection via region-based fully convolutional networks. In: Advances in Neural Information Processing Systems **29**. (2016)
31. Hoiem, D., Chodpathumwan, Y., Dai, Q.: Diagnosing error in object detectors. In: European Conference on Computer Vision. (2013)
32. Russakovsky, O., Deng, J., Su, H., Krause, J., Satheesh, S., Ma, S., Huang, Z., Karpathy, A., Khosla, A., Bernstein, M.: Imagenet large scale visual recognition challenge. International Journal of Computer Vision **115**(3) (2015) 211–252
33. Huang, G., Liu, Z., Maaten, L.V.D., Weinberger, K.Q.: Densely connected convolutional networks. CoRR **abs/1608.06993** (2016)